**Supporting Information**

# Membrane-Separated Electrochemical Latrine Wastewater Treatment

Yang Yang,[a] Lin Lin,[b] Leda Katebian Tse,[a] Heng Dong,[c] Shaokun Yu,[d]

and Michael R. Hoffmann*[a]

[a] Division of Engineering and Applied Science, Linde-Robinson Laboratory, California Institute of Technology, Pasadena, California, 91125, United States

[b] Environmental Engineering Research Centre, Department of Civil Engineering, The University of Hong Kong, Hong Kong, China

[c] State Key Joint Laboratory of Environment Simulation and Pollution Control, School of Environment, Tsinghua University, Beijing 100084, PR China

[d] Department of Civil & Environmental Engineering, University of California, Davis, California 95616, United States

**Text S1**

**Inactivation of *Ascaris Suum* eggs**

*Ascaris suum* eggs purchased from Excelsior Sentinel, Inc (Ithaca, NY) were isolated from the intestines of infected pigs. Eggs were shipped at concentration of approximately $10^5$/ml and stored at 4°C in 0.1N sulfuric acid to prevent growth of fungi and bacteria. Prior to experiments, eggs were removed from the stock solution by filtration (filter paper 413, VWR). Eggs were then re-suspended in latrine wastewater to give a starting concentration of approximately 100-200 eggs/ml. Electrolysis experiments were carried out for 4 hours using membrane-less and CEM configurations described in the above sections. In CEM experiments, the membrane was soaked and vortexed into treated latrine wastewater to remove any eggs accumulated onto the membrane surface. To confirm the mechanism that led to *Ascaris suum* inactivation, eggs were also subjected to membrane-less electrolysis at pH 8.8 (without regulation) and 1.5 (acidified by 1 M $H_2SO_4$).

*Ascaris suum* viability was determined using the Live/Dead BacLight kit (Invitrogen Molecular Probes) adapted from previous research.[1-3] STYO 9 (green) is a cell-permeable nucleic acid dye that targets viable eggs while propidium iodide (red) is a nucleic acid dye that stains inactivated eggs. At the start and end of each experiment, 1 ml of sample was taken from the electrolysis chamber. 4 µl of the combined stains (1:1) were added to the 1 ml sample and incubated in the dark for 15 min with mixing. The stained sample was added to a microscope slide chamber (Nunc Lab-Teck) and observed under fluorescence microscopy (DMi8, Leica) using 4x and 10x magnification at an excitation of 490 ±920nm (STYO 9) and 575 ± 30 nm (propidium iodide). The numbers of viable (live) and inactivated (dead) eggs were counted at 4x magnification over the whole chamber area (~25 images for 1 ml sample) using the cell-counter plugin in Image J.

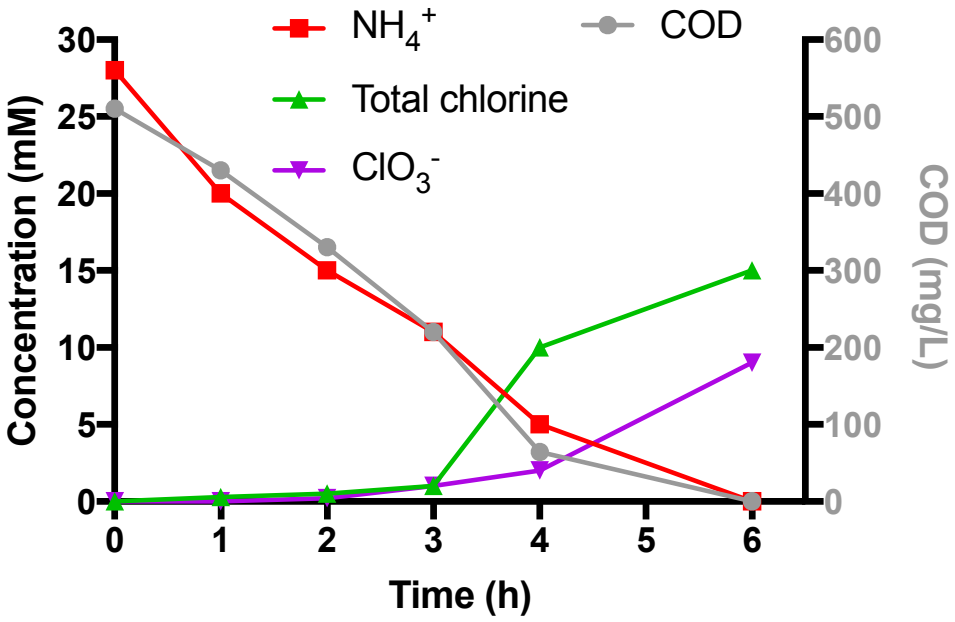


**Fig. S1** Membrane-free electrolysis of latrine wastewater with a STI anode at 25 mA/cm$^2$.

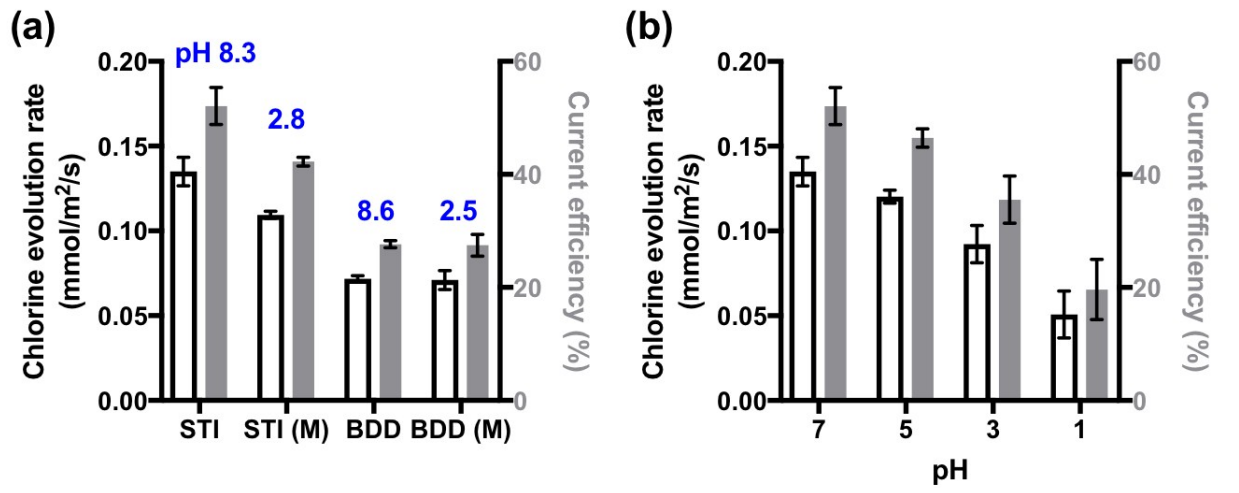


**Fig. S2** a) Chlorine evolution rate and current efficiency measured in different cell configurations. b) Impact of pH on chlorine evolution performance of STI anode. For all the tests, 50 mM NaCl was used as electrolyte and the applied current density is 5 mA/cm$^2$. The measurement lasts for 15 min. The blue texts shown in **Figure S1a** are pH of anolyte measured after 15 min of electrolysis.

Electrolyte used for chlorine evolution rate (CER) measurement is 50 mM NaCl. The current efficiency was estimated using the following equation:

$$\eta = \frac{2VFd[\mathrm{FC}]}{Idt} \quad (1)$$

where $V$ is electrolyte volume (25 mL), $F$ is the Faraday constant 96485 C mol$^{-1}$, $I$ is the current (A).

The chlorine evolution rate on the STI anode as a function of pH shows that there is a substantial decrease in the rate of chlorine evolution with pH (**Figure S2b**). At low pH, the number of catalytically active surface hydroxyl group sites (e.g., 4 to 5 >SnOH groups per nm$^2$) is decreased due to protonation (e.g., for $SnO_2$ $pH_{zpc}$ = 4.5, there will be more $>SnOH_2^+$ sites versus the neutral >SnOH sites ).[4] In a CEM-divided cell, the cathodic reduction of chlorine should be excluded. However, this potential positive effect is offset by the lower pH of the anodic cell during membrane-separated electrolysis (**Figure S2a**).

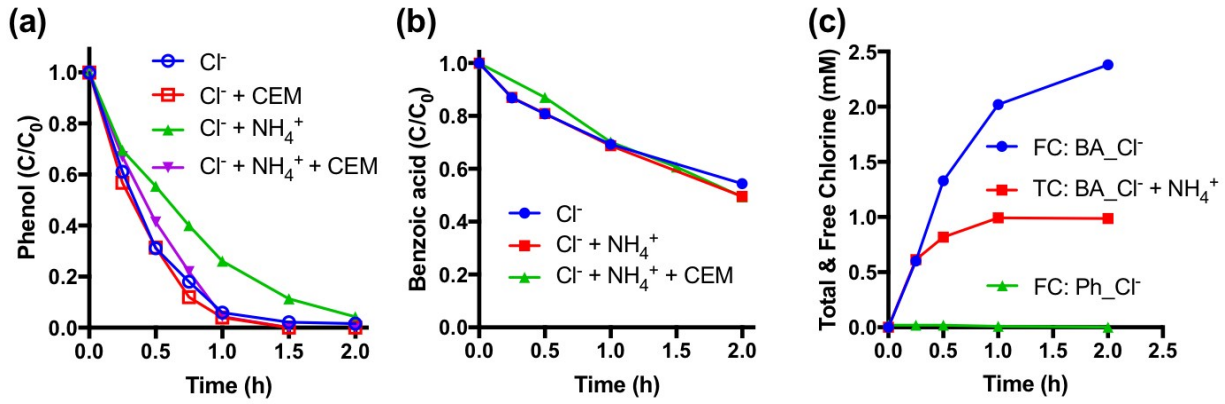


**Fig. S3** a) Phenol degradation by STI anode. b) Benzoic acid degradation by BDD anode. c) Concentration of total chlorine (TC) and free chlorine (FC) as functions of electrolysis duration. All tests were conducted in 50 mM NaCl at 5 mA/cm$^2$. In some tests, 50 mM $NH_4ClO_4$ was added.

The electrolysis of Phenol (Ph, 2 mM) by STI anode was selected as a model of chlorine-mediated electrochemical oxidation reaction. The electrolysis of benzoic acid (BA, 2 mM) was chosen to study the radical-mediated electrochemical oxidation, because the BA can only be oxidized by radicals.[5,6] As shown in **Fig. S3b**, the decay rate of BA on BDD anode is not affected by the addition of 50 mM $NH_4^+$. This implies that radical-mediated oxidation is barely affected by $NH_4^+$, which again support the fact that BDD is more efficient for organic removal in latrine wastewater. In contrast, the phenol degradation on STI anode is slower in the presence of $NH_4^+$, indicating that $NH_4^+$ significantly suppress the chlorine-mediated oxidation (**Fig. S3a**).

As shown in **Fig. S3c**, free chlorine cannot be detected in chlorine mediated phenol oxidation by STI anode. Same result is observed in the Ph oxidation in the presence of $NH_4^+$ (data not shown). However, chlorine production is significant in radical mediate BA oxidation by BDD anode. A negative impact of $NH_4^+$ on chlorine production is observed. These results are in line with the latrine wastewater electrolysis, showing that both easily degradable organics and $NH_4^+$ can rapidly deplete chlorine.

**Fig. S3a** shows that the CEM assisted electrolysis by STI anode excludes the inhibitive effect of $NH_4^+$ on chlorine mediated oxidation, as the decay rate of phenol is commensurate with that observed in membrane-less electrolysis in the absence of $NH_4^+$.

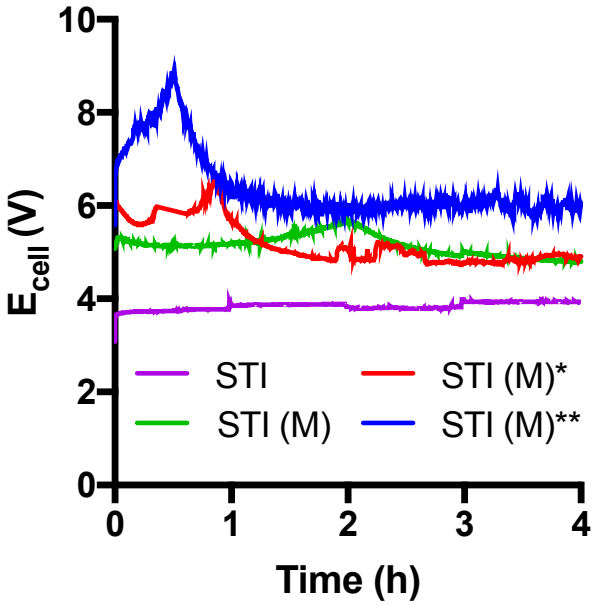


**Fig. S4** Cell voltage as a function of electrolysis time. Tests marked with "M" were performed in CEM electrolysis. All the electrolysis tests were conducted at 5 mA/cm$^2$, except STI (M)* and STI (M)** were operated at 10 and 15 mA/cm$^2$, respectively.

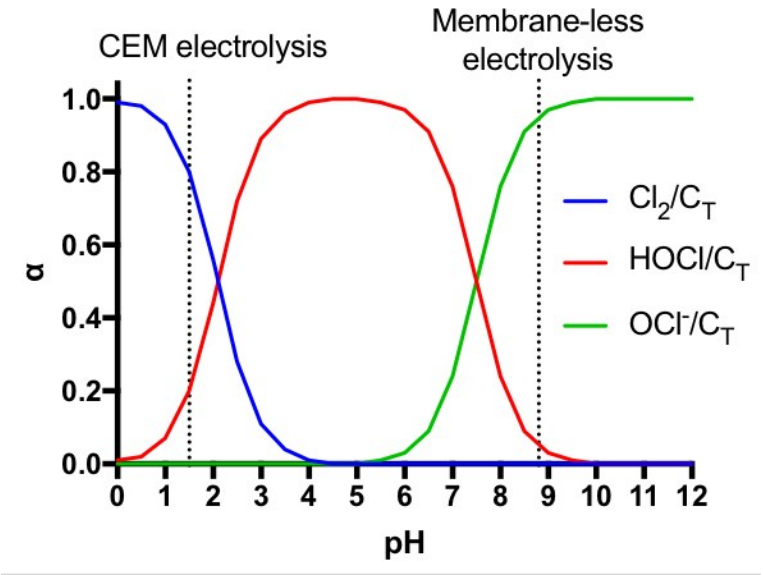


**Fig. S5** Distribution diagram of chlorine species as a function of pH. $[Cl^-]$ = 50 mM, $C_T = [Cl_2] + [HOCl] + [OCl^-]$.

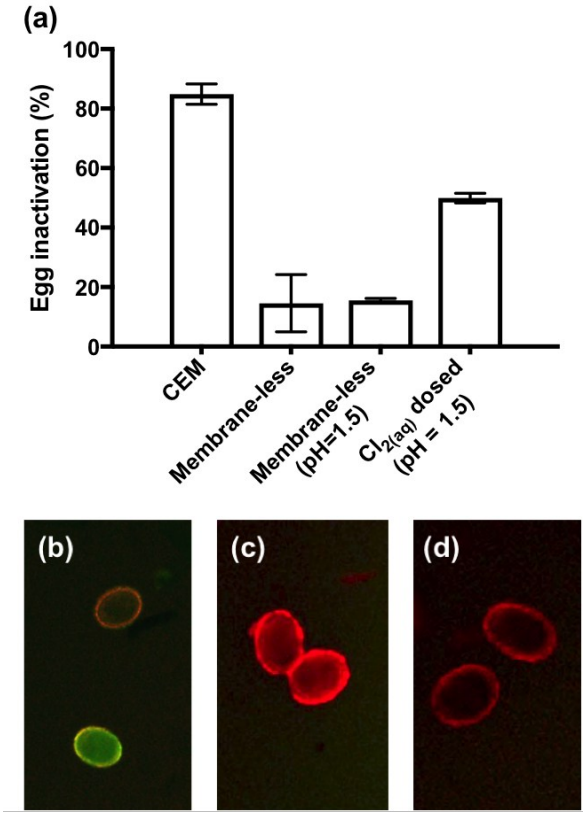


**Figure S6.** a) Percent of *Ascaris suum* eggs inactivated after 4 hours of CEM and membrane-less electrolysis. Microscope images at 10x magnification depicting b) viable eggs as those stained with STYO 9 (cell-permeable) and the eggshell stained with both STYO-9 and propidium iodide. Inactivated eggs observed in c) CEM separated electrolysis and d) membrane-free electrolysis at pH of 1.5. Since propidium iodide is not-cell permeable, the dye can only penetrate the egg if the inner lipoprotein layer was damaged as noted in past research.[3] Therefore, eggs were considered to be inactivated if stained completely with propidium iodide showing red fluorescence.

The experimental procedure of homogeneous $Cl_{2(aq)}$ oxidation is described as follows: First, 45 mM NaClO was added to the latrine wastewater to deplete the $NH_4^+$ (30 mM) via breakpoint chlorination. After that, additional 5 mM NaClO was dosed into the solution, following by the adjustment of the pH to 1.5 to produce 5 mM $Cl_{2(aq)}$. Then helminth eggs were dosed into the amended wastewater, samples were taken after 4 h reaction.

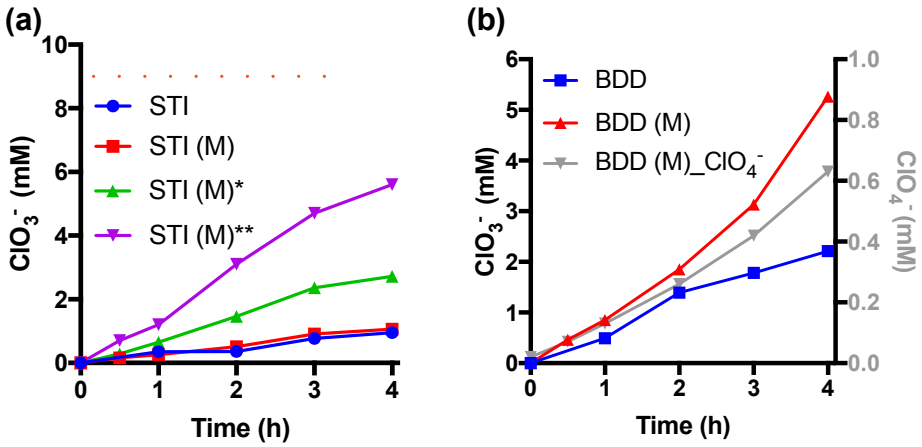


**Fig. S7** Formation of $ClO_3^-$ and $ClO_4^-$ in wastewater electrolysis by a) STI and b) BDD anodes. Dash line in **Figure S7a** shows the $[ClO_3^-]$ = 9 mM detected after 6 h of membrane-free electrolysis by STI anode at 25 mA/cm$^2$, in which the complete removal of COD and $NH_4^+$ was obtained (**Fig. S1**).

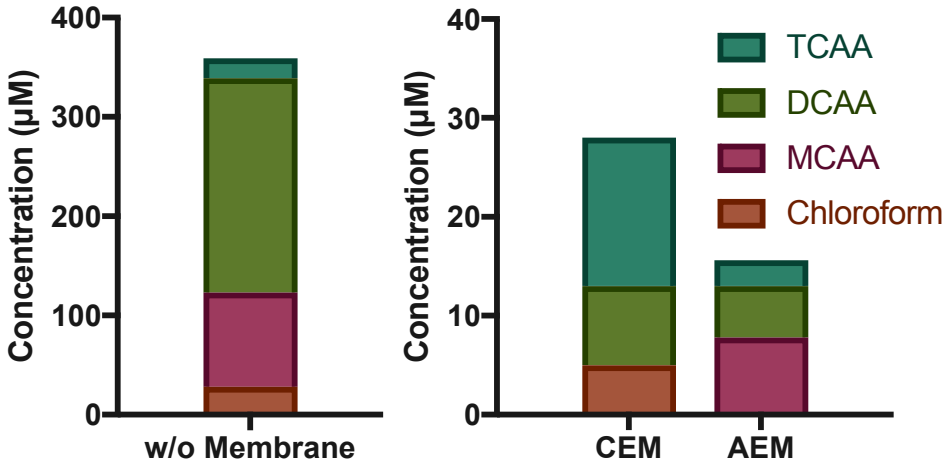


**Fig. S8** Concentration profiles of THMs and HAAs in effluent of membrane-free and membrane electrolysis. Membrane-free electrolysis was operated for 6 h at 25 mA/cm$^2$. CEM electrolysis was performed for 4 h at 15 mA/cm$^2$. AEM electrolysis was conducted for 1.5 h at 6 V.

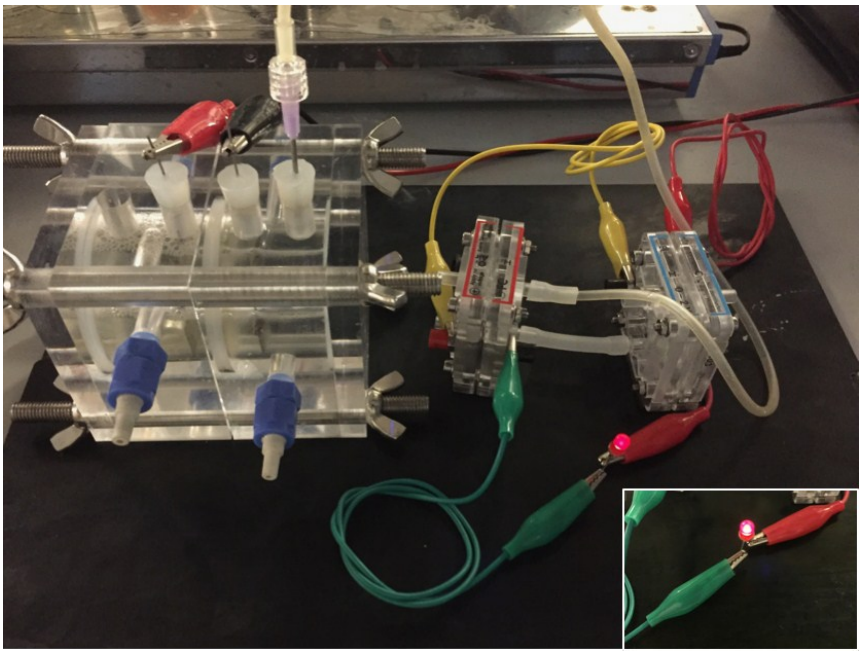

**Fig. S9** The utilization of cathodically produced $H_2$ by fuel cell. Hydrogen gas was passed through the anodic chamber of two mini hydrogen/air fuel cell (FuelCellStore). The cathodic chambers of the fuel cells were exposed to air. Each fuel cell could generate 1 V open-circuit potential. Two mini fuel cells connected in series is able to light up a red LED lamp (Microtivity).

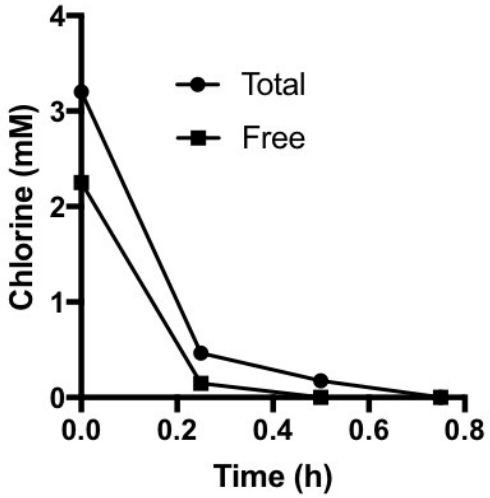


**Fig. S10** Cathodic reduction of total and free chlorine in the treated wastewater by AEM electrolysis.

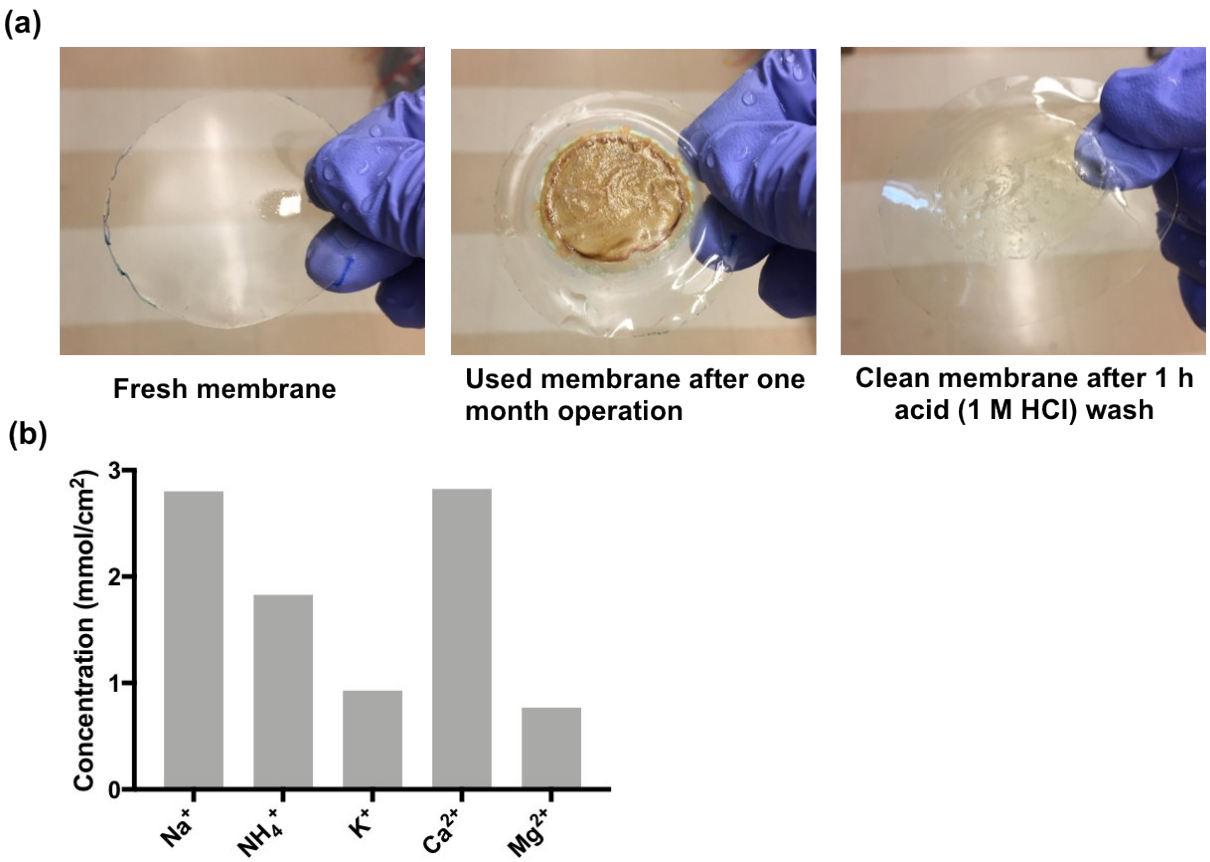


**Figure S11**. a) Photos of fresh, used, regenerated Nafion membrane. Foulant can be completely removed by acid wash. The wrinkle on the washed membrane is due to the deformation during cell assembling. b) Ionic species detected in the HCl wash solution. $Ca^{2+}$ and $Mg^{2+}$ are responsible for the fouling, while $Na^{+}$, $K^{+}$, and $NH_4^{+}$ are ionic species trapped in the membrane.

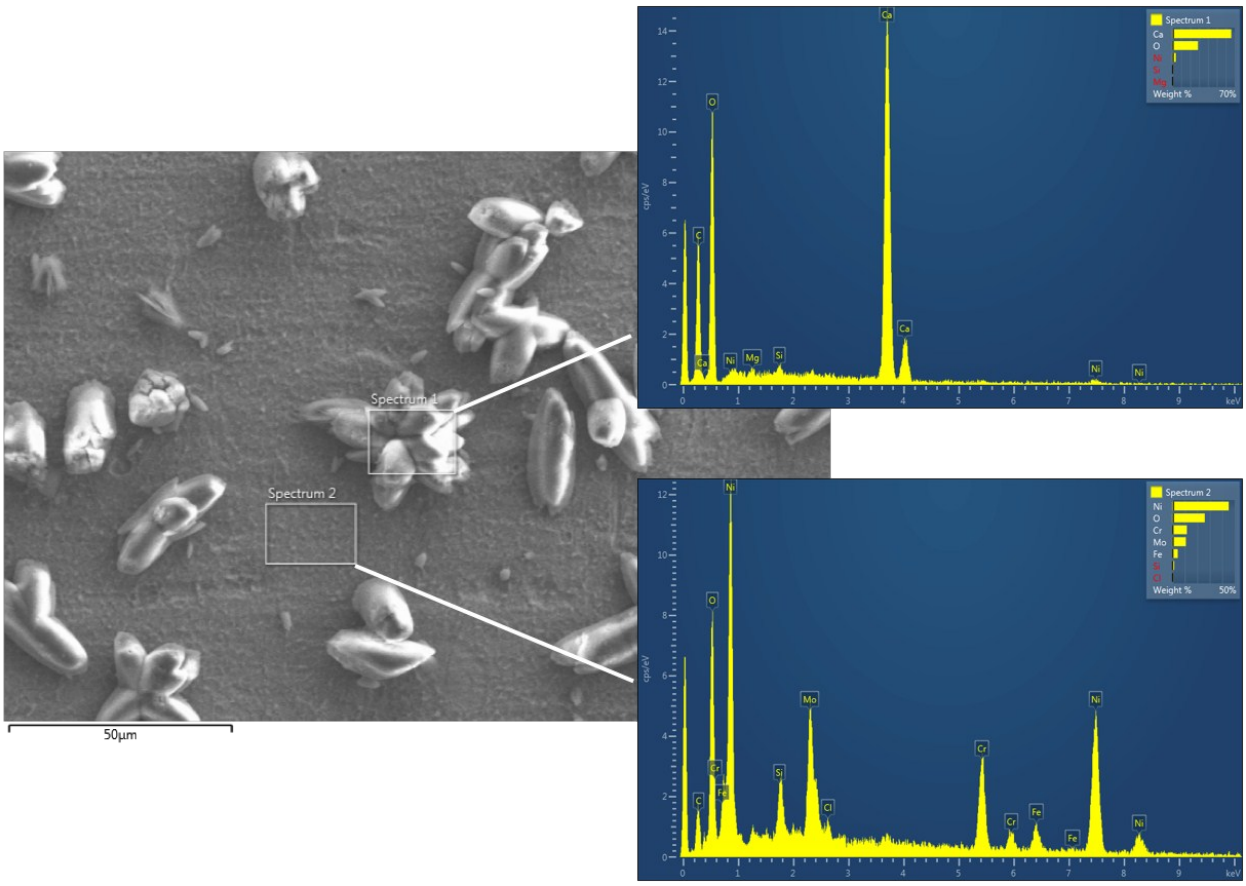


**Fig. S12.** SEM-EDS analyses of scaled (upper right) and unscaled area (lower right) of cathode after one-month CEM electrolysis. The scale comprises of Ca and Mg precipitate. The unscaled area is the surface of stainless-steel featuring Fe, Co, and Ni as the dominant elements.

**Table S1**. Summary of electrochemical oxidation studies for the treatment of actual wastewater.

| Water treated | Anode | Membr. | Max. efficiency for COD & $NH_4^+$ removal | Energy consumption (kWh/kg COD) | Nutrient recovery | Disinfection | Investigated byproducts[a] | $H_2$ Conc. (%) | Roles of membrane | Stability test | Ref |
|---|---|---|---|---|---|---|---|---|---|---|---|
| ROC | BDD Ru/Ti | none | COD: > 90% $NH_4^+$: > 90% | 83-425 | NA | NA | $ClO_3^-$ | NA | NA | NA | 7 |
| ROC | BDD | none | COD: >90% | 290-340 | NA | NA | AOX, THMs, HAAs | NA | NA | NA | 8 |
| ROC | BDD | None | COD: > 90% $NH_4^+$: > 90% | 59 | NA | NA | THMs | NA | NA | NA | 7 |
| ROC | Ir/Ti | CEM | COD: 15% $NH_4^+$: 30% | *ca.* 170 | NA | NA | THMs; HAAs | NA | NA | NA | 9 |
| ROC | Sn/Ti Pt-Ir/Ti BDD | CEM | COD: >90% | NA | NA | NA | THMs | NA | NA | NA | 10 |
| ROC | BDD | CEM, none | COD: > 90% | 250-340 | NA | NA | AOX | NA | Increase energy consumption | NA | 11 |
| Landfill | Pb/Ti | CEM, none | TOC: 45.6% | NA | NA | NA | AOX | NA | Enhance TOC removal | NA | 12 |
| Landfill | BDD | none | COD: 0.6-19% $NH_4^+$: 11% | 134 | NA | NA | THMs, HANs HKs, DCA | NA | NA | NA | 13 |
| Domestic | BDD | CEM | COD: > 90% | NA | NA | NA | AOX; $ClO_3^-$; $ClO_4^-$ | NA | NA | NA | 14 |
| Urine | BDD, Ir | none | COD: 75% $NH_4^+$: < 20% | NA | NA | NA | chlorinated methanes, DCA, $ClO_3^-$, $ClO_4^-$ | NA | NA | NA | 15 |
| Urine | Ir/Ti | CEM | NA | NA | $NH_3$ | NA | NA | NA | $NH_4^+$ recovery | NA | 16-18 |
| Latrine | BiTi/Ir | none | COD: > 90% $NH_4^+$: > 90% | 96 | NA | *E. Coli.* | NA | 35-60 | NA | NA | 19 |
| Latrine | Sn/Ti/Ir | none | COD: > 90% $NH_4^+$: > 90% | 370 | NA | NA | NA | NA | NA | NA | 20 |
| **Latrine** | **BDD Sn/Ti/Ir** | **CEM, AEM, none** | **COD: > 90% $NH_4^+$: > 90%** | **40-92** | **$NH_3$, $PO_4^{3-}$** | **Helminth eggs** | **THMs, HAAs, $ClO_3^-$, $ClO_4^-$** | **100** | **Recover $NH_4^+$ and $PO_4^{3-}$ Enhance COD removal Enhance deactivation Pure $H_2$ production Reduce energy consumption** | **One month** | **This study** |

[a] trihalomethanes (THMs), haloacetic acid (HAAs) haloacetonitriles (HANs), haloketons (HKs), 1,2-dichloroethane (DCA), and Adsorbable organic halogen (AOX).

**Table S2.** Composition of latrine wastewater

| property | latrine wastewater |
|---|---|
| pH | 8.8 |
| conductivity (mS/cm) | 11.5 |
| COD (mg $O_2$/L) | 550 ± 40 |
| $NH_4^+$ (mM) | 28 ± 4 |
| $Cl^-$ (mM) | 50 |
| $Br^-$ (μM) | 3 |
| $PO_4^{3-}$ (mM) | 3.4 |
| $Ca^{2+}$ (mM) | 1 |
| $Mg^{2+}$ (mM) | 1.2 |

**References**


1. J. Dabrowska, J. Zdybel, J. Karamon, M. Kochanowski, K. Stojecki, T. Cencek and T. Klapec, Assessment of viability of the nematode eggs (Ascaris, Toxocara, Trichuris) in sewage sludge with the use of LIVE/DEAD Bacterial Viability Kit, *Ann. Agric. Environ. Med.*, 2014, **21**.
2. A. Karkashan, B. Khallaf, J. Morris, N. Thurbon, D. Rouch, S. R. Smith and M. Deighton, Comparison of methodologies for enumerating and detecting the viability of Ascaris eggs in sewage sludge by standard incubation-microscopy, the BacLight Live/Dead viability assay and other vital dyes, *Water Res.*, 2015, **68**, 533-544.
3. M. Włodarczyk, J. Zdybel, M. Próchniak, Z. Osiński, J. Karamon, T. Kłapeć and T. Cencek, Viability assessment of Ascaris suum eggs stained with fluorescent dyes using digital colorimetric analysis, *Exp. Parasitol.*, 2017, **178**, 7-13.
4. V. Consonni, S. Trasatti, F. Pollak and W. O'Grady, Mechanism of Chlorine Evolution on Oxide Anodes Study of pH Effects, *J. Electroanal. Chem. Interfacial Electrochem.*, 1987, **228**, 393-406.
5. H. Park, C. D. Vecitis and M. R. Hoffmann, Electrochemical Water Splitting Coupled with Organic Compound Oxidation: The role of Active Chlorine Species, *J. Phys. Chem. B*, 2009, **113**, 7935-7945.
6. J. Fang, Y. Fu and C. Shang, The Roles of Reactive Species in Micropollutant Degradation in the UV/free Chlorine System, *Environ. Sci. Technol*, 2014, **48**, 1859-1868.
7. G. Pérez, A. R. Fernández-Alba, A. M. Urtiaga and I. Ortiz, Electro-oxidation of reverse osmosis concentrates generated in tertiary water treatment, *Wat. Res.*, 2010, **44**, 2763-2772.
8. A. Y. Bagastyo, D. J. Batstone, I. Kristiana, W. Gernjak, C. Joll and J. Radjenovic, Electrochemical Oxidation of Reverse Osmosis Concentrate on Boron-Doped Diamond Anodes at Circumneutral and Acidic pH, *Wat. Res.*, 2012, **46**, 6104-6112.
9. A. Y. Bagastyo, J. Radjenovic, Y. Mu, R. A. Rozendal, D. J. Batstone and K. Rabaey, Electrochemical oxidation of reverse osmosis concentrate on mixed metal oxide (MMO) titanium coated electrodes, *Wat. Res.*, 2011, **45**, 4951-4959.

10. A. Y. Bagastyo, D. J. Batstone, K. Rabaey and J. Radjenovic, Electrochemical Oxidation of Electrodialysed Reverse Osmosis Concentrate on Ti/Pt-IrO2, Ti/SnO2-Sb and Boron-doped Diamond Electrodes, *Wat. Res.*, 2013, **47**, 242-250.
11. A. Y. Bagastyo, D. J. Batstone, I. Kristiana, B. I. Escher, C. Joll and J. Radjenovic, Electrochemical Treatment of Reverse Osmosis Concentrate on Boron-Doped Electrodes in Undivided and Divided Cell Configurations, *J. Hazard. Mater.*, 2014, **279**, 111-116.
12. Y. Lei, Z. Shen, R. Huang and W. Wang, Treatment of landfill leachate by combined aged-refuse bioreactor and electro-oxidation, *Wat. Res.*, 2007, **41**, 2417-2426.
13. Á. Anglada, A. Urtiaga, I. Ortiz, D. Mantzavinos and E. Diamadopoulos, Boron-doped diamond anodic treatment of landfill leachate: Evaluation of operating variables and formation of oxidation by-products, *Wat. Res.*, 2011, **45**, 828-838.
14. S. Garcia-Segura, J. Keller, E. Brillas and J. Radjenovic, Removal of organic contaminants from secondary effluent by anodic oxidation with a boron-doped diamond anode as tertiary treatment, *J. Hazard. Mater.*, 2015, **283**, 551-557.
15. H. Zöllig, A. Remmele, C. Fritzsche, E. Morgenroth and K. Udert, Formation of Chlorination Byproducts and Their Emission Pathways in Chlorine Mediated Electro-oxidation of Urine on Active and Nonactive Type Anodes, *Environ. Sci. Technol.*, 2015, **49**, 1062-11069.
16. W. A. Tarpeh, J. M. Barazesh, T. Y. Cath and K. L. Nelson, Electrochemical stripping to recover nitrogen from source-separated urine, *Environ. Sci. Technol.*, 2018, **52**, 1453-1460.
17. M. E. Christiaens, S. Gildemyn, S. Matassa, T. Ysebaert, J. De Vrieze and K. Rabaey, Electrochemical Ammonia Recovery from Source-Separated Urine for Microbial Protein Production, *Environ. Sci. Technol.*, 2017.
18. A. K. Luther, J. Desloover, D. E. Fennell and K. Rabaey, Electrochemically driven extraction and recovery of ammonia from human urine, *Wat. Res.*, 2015, **87**, 367-377.
19. K. Cho, Y. Qu, D. Kwon, H. Zhang, C. m. A. Cid, A. Aryanfar and M. R. Hoffmann, Effects of Anodic Potential and Chloride Ion on Overall Reactivity in Electrochemical Reactors Designed for Solar-Powered Wastewater Treatment, *Environ. Sci. Technol.*, 2014, **48**, 2377-2384.

20. Y. Yang, J. Shin, J. T. Jasper and M. R. Hoffmann, Multilayer Heterojunction Anodes for Saline Wastewater Treatment: Design Strategies and Reactive Species Generation Mechanisms, *Environ. Sci. Technol.*, 2016, **50**, 8780-8787.